Detection beyond the Debye's length with an electrolyte gated organic field-effect transistor

Gerardo Palazzo[*], *Donato De Tullio, Maria Magliulo, Antonia Mallardi, Francesca Intranuovo, Mohamed Yusuf Mulla, Pietro Favia, Inger Vikholm-Lundin,* and *Luisa Torsi*

[*] Prof. G.P. Corresponding-Author,

prof. G. Palazzo, Dr. D. De Tullio, Dr. M. Magliulo, Dr. F. Intranuovo, Dr. M.Y. Mulla, Prof. P. Favia, Prof. L. Torsi, Dipartimento di Chimica, Università degli Studi di Bari Aldo Moro, Via Orabona 4
70126, Bari (Italy)
E-mail: gerardo.palazzo@uniba,it;

A. Mallardi
CNR-IPCF, Istituto per i Processi Chimico-Fisici Via Orabona 4
70126, Bari (Italy)

I. Vikholm-Lundin
University of Tampere, BioMediTech, Tampere, IBT FI-33014, Finland

BioMediTech, University of Tampere, and Fimlab Laboratories, Tampere, Finland

Keywords: Organic Bio-Electronic Sensing; Electrolyte Gated Organic Field-Effect Transistors; Donnan Equilibria; Electrostatic Double Layer.

Portable and easy to operate sensors for diseases markers would be ideal for point-of-care applications. Low-cost and high performance add up if transducers such as organic field-effect transistors (OFETs) are used.[1,2,3] These organic electronic sensors, proven to be extremely sensitive,[4,5] can be endowed with selectivity by using biomolecules as receptor deputed to recognize a target molecule. As an aqueous electrolyte solution is the natural environment for biological receptors, presently the challenge is to develop OFET *bio*-sensors that, besides integrating biomolecules, can also operate in an aqueous electrolyte. To date, different architectures sharing similar basic operational principles, have been proposed.[6,7] A layer of receptors is linked to one of the transistor electronic active interfaces and the

interaction with a target molecule affects the device output current. In an electrolyte-gated field-effect transistor (EGOFET)[8, 9] the gate-electrode/electrolyte[10] and the electrolyte/organic-semiconductor[11] interfaces can be modified with the deposition of bio-receptors. The ligand binding to the receptor changes the receptor conformation and/or the charge distribution at the bio-modified interface, eventually causing a shift of the transistor threshold voltage (V_T) or impacting on the product between field-effect mobility and the gating system capacitance per unit area term ($\mu_{FET} \cdot C$).

Electrostatic interactions in an electrolyte solution are known to extend at most to the Debye's screening length λ.[12] This defines the length-scale at which a charged analyte can be electrically probed at the detector interface. Indeed, if a charge resides at a distance further off than λ, it is shielded by the ions of the electrolyte solution. Some reports can be found that show how OFET and nanowire FET sensors become "blind" to the target molecule (analyte) when the Debye's length is below the distance at which the recognition event takes place.[13,14,15] In general, these contributions suggest that OFET detections were possible only at salt concentration low enough so that λ is larger than the analyte size.[13] Lately however, few reports have evidenced how EGOFET biosensing can be performed even when a target species is confined beyond λ,[11,16,17] apparently in contrast with the Debye's length rule.
To clarify this issue on the basic functional mechanisms of a Bio-EGOFET, a systematic study of a sensor response as a function of the Debye's length, the receptor charge and the distance at which the binding event takes place, is here reported. Strikingly a Bio-EGOFET sensor is shown to successfully detect binding events occurring at 30 λs from the transistor electronic channel and even to deliver higher responses at low λs or equivalently in the presence of high salt concentrations.

OFETs are three terminals devices comprising a source (S) and a drain (D) contact separated by an organic semiconductor (OSC) layer. This is addressed as the electronic channel region of the device. The third terminal, the gate (G), is separated from the OSC by a dielectric medium. The device is operated in the common source configuration[6] and, for a p-type OSC (Poly-3-hexylthiophene, P3HT, in the present study), the negative bias applied between the gate and the grounded source (V_G) leads to the accumulation of positive charges at the interface between the OSC and the dielectric. Under a negative source-drain bias, V_{DS}, a negative current I_{DS}, whose intensity is a function of the applied V_G and of the gating system capacitance C, flows in the channel. Learning the lesson from electrolytic supercapacitors, high-capacitance gate dielectrics have been used where the charge separation is achieved through the formation of Helmholtz double layers,[8] few Å thick, at the interfaces between the electrolyte solution and the OSC as well as between the electrolyte and the gate contact (**Figure 1a)**. Upon application of V_G, anions and cations migrate in opposite directions, leading to a net charge accumulation at the elicited two electronically active interfaces leaving a neutral electrolyte in between. With a sufficiently large gate contact, the applied voltage fully drops across the HDLs generating a capacitance as high as 10 μF/cm^2. This strictly holds only in the presence of the high ions concentrations found in ionic liquids and solid polyelectrolytes. In conventional electrolyte solutions, only a fraction of the charges are confined at the HDLs, the residual aliquot forms the Gouy-Chapman diffuse double layers (GCDLs) with a capacitance that is inversely proportional to the Debye's screening length, defined as:[12]

$$\lambda = \sqrt{\frac{\varepsilon\varepsilon_0 KT}{e^2 \sum_j z_j{}^2 c_j}} \qquad (1)$$

where ε is the relative dielectric constant of the medium, ε_0 the vacuum permittivity, *e* the elementary charge, KT the thermal energy and the summation is twice the solution ionic strength , i_s with z_j and c_j being the valence and the concentration of the *j*-th ion respectively.

The GCDL capacitance per unit area is $C_{GCDL} = \frac{\varepsilon\varepsilon_0}{\lambda} cosh\left(\frac{ze\Phi^\circ}{2KT}\right)$ that for low surface potential (Φ°) reduces to:[12]

$$C_{GCDL} = \frac{\varepsilon\varepsilon_0}{\lambda} = \sqrt{\frac{\varepsilon\varepsilon_0}{KT}} e\sqrt{i_s} \qquad (2).$$

The total capacitance of the electrolyte gating system C, can be described, at first instance, as the HDLs and GCDLs capacitors in series dominated by the smaller one, namely by C_{GCDL}. This latter term is proportional to $\sqrt{i_s}$ meaning that, working with dilute electrolyte solutions will invariably result in a smaller gate capacitance leading to lower output currents and worse electronic performances. If it was true that large λ values were mandatory for a highly performing sensing, as previously claimed, this occurrence would have been prejudicial for the use of EGOFETs as biosensors.

To investigate this issue the Bio-EGOFET sensing platform comprising a bio-layer at the interface between the OSC and the electrolyte (**Figure 1a)**,[11] was used. The bio-layer is composed of a phospholipid bilayer (PL) covalently anchored to the OSC surface through a plasma-deposited -COOH functionalized thin coating. Some of the anchored PLs are endowed with a biotin moiety, having an incomparably high binding affinity for streptavidin (SA) or avidin (AV) proteins.[18] Both proteins hold four binding sites, are similar in size (~ 5nm) but have opposite charges: SA is negatively and the AV is positively charged at the operating pH of 7.4. The binding of the negatively (positively) charged SA (AV) to the biotinylated phospholipid bilayer results in the PL/SA(AV) staked layer (**Figure 1a**). whose deposition and characterization was previously detailed [11]. After binding to PL, SA and AV, have empty binding sites available to bind a biotinylated anti-body (Ab) leading to the PL/SA(AV)/Ab multilayer (**Figure 1a**). Here, the antibody against the C-reactive protein (CRP) was used, it is negatively charged and has a size of ~ 15 nm. The Ab selectively binds the CRP, a large (~ 10

nm) negatively charged protein that is rising a great deal of interest as marker in cardiovascular diseases as wells as a prognostic indicator in gastroesophageal cancer. The binding of CRP to the PL/SA(AV)/Ab gives rise to a three stacked proteins system addressed as: PL/SA(AV)/Ab/CRP (**Figure 1a**). Such bio-multilayers have been conceived to allow the electronic probing of a binding event occurring at different distances from the surface of the phospholipids bilayer; namely λ=20 nm for the Ab binding to PL/SA(AV), λ=30 nm for the CRP binding to PL/SA(AV)/Ab.

The protein coverage of the OSC surface was optimized by means of a surface plasmon resonance (SPR) study performed on PL bilayers characterized by a different ratio, *R,* of biotinylated PL *vs.* total PL composition. The results are shown in **Figure 1b** where the binding of avidin to a PL layer (black dots) saturates at *R*=1/33 corresponding to 23 nm^2 per AV unit in agreement with the maximum AV packing reported on silica.[19] The binding of Ab to PL/AV (red dots) saturates at a lower *R*-value (1/50 *i.e.* 50 nm^2 per Ab) reflecting the larger area occupied by an Ab. Finally, the large CRP pentameric complex (blue symbols) saturates at *R*=1/100 (70 nm^2 per CRP). In view of the use of this multilayer for CRP detection, a PL layer with *R*=1/100 was chosen to assure the full CRP coverage. The measurements reported in **Figure 1b** were performed in a phosphate buffered saline (PBS) solution (pH= 7.4) with a high ionic strength, i_s= 0.163 M, mimicking the ionic composition of body fluids, that results in a Debye's length, λ, as short as 0.7 nm.

The same medium was used to gate the EGOFETs integrating the three multilayers sketched in **Figure 1a.** The I_{DS} fractional changes upon formation of a new layer are shown in **Figure 1c**. As already described[20], the binding of the SA or AV gives rise to opposite effects on I_{DS}. The SA binding to the PL bilayer induces a, previously reported[11], current increase while the

AV binding provokes a current decrease. These effect are usually rationalized in terms of the opposite protein charges.[13,20]

Interestingly, the subsequent formation of the PL/SA(AV)/Ab and PL/SA(AV)/Ab/CRP multi-layers, gives rise to current changes that are independent from the charge of the protein laying underneath: the binding of Ab always causes a current decrease while CRP loading always makes the output signal to increase. These features give evidence that the binding of the proteins to the outermost bio-layer determines the EGOFET response.

These experiments provide the background knowledge to perform a proof-of-principle for an important applicative fall-out. Indeed, the measurements described so far were performed at i_s values typical for human blood, suggesting that Bio-EGOFETs could be used to sense analytes directly in a body fluid. The PL/SA/Ab EGOFET was therefore tested as sensor for CRP detection directly in human serum. The transfer characteristics reported in **Figure 1d** clearly demonstrate that an I_{DS} sizable increase can be measured upon exposure of the bio-EGOFET to human serum added with clinically relevant concentrations of CRP.

To rationalize the sensing mechanism, the cumulative response-dose curves for the binding of Ab and CRP were measured. The response was taken as the fractional I_{DS} change after incubation of the device in a solution of the ligand at a given concentration. The response is therefore $\Delta I/I_0 = (I_{DS}-I_0)/I_0$ with I_0 being the I_{DS} base-line measured with a solution deprived of the target molecule. The cumulative responses, reported as blue dots in **Figure 2a** and **2b,** have been obtained by exposing the same EGOFET device to solutions of increasing protein concentrations. **Figure 2a** shows the binding of Ab to PL/SA leading to a *decrease* in the response. At variance, loading PL/SA/Ab with CRP results in a response increases (**Figure 2b**). The data of **Figure 2** refer to replicates (at least three) obtained on different transistors fabricated on the same chip, thus are representative of intra-device reproducibility. The

behaviour has been confirmed over several tents of devices prepared with different batches of P3HT, proteins and PL. The data of **Figure 2a** and **2b** reveal the following unexpected and peculiar features:

i) it is possible to measure a response associated to a binding event taking place at a distance of 20-30 nm (30-40 λ) from the transistor channel.;

ii) the electronic transduction is dominated by the outermost protein in the staked layer and not by those residing underneath, though these are closer to the device electronic channel.

An explanation for the reported evidences can be given by studying the capacitance and the V_T changes occurring upon binding. The transfer characteristics are measured in the saturation regime, $V_{DS}>(V_G - V_T)$, where the I_{DS} is given by:

$$I_{DS} = \frac{W}{2L} C\mu_{FET} \cdot (V_G - V_T)^2 \qquad (3)$$

where W and L are the width and the length of the channel. According to equation (3), V_T and the $C\cdot\mu_{FET}$ product can be independently evaluated by the linear interpolation of $\sqrt{I_{DS}}$ *vs.* V_G. [6] The Bio-EGOFET response can be written, decoupling the capacitance and the threshold voltage contributions, as:

$$\frac{\Delta I}{I_0} = \frac{\Delta C}{C_0} + \frac{2\Delta V_T}{(V_G - V_{T,0})} \qquad \mathbf{(4)}$$

where the subscript 0 denotes the system chosen as base-line. As the binding events take place far from the OSC channel, it is assumed that μ_{FET} stays constant. The V_T and C contributions to the response upon Ab binding to PL/SA and upon CRP binding to PL/SA/Ab are also shown in **Figure 2a** and **Figure 2b**, respectively. The comparison between V_T and C contribution to the $\Delta I/I_0$ values, demonstrates that the response to the analyte is mainly capacitive. To rationalize this capacitive behavior, the polyelectrolyte nature of the stacking multi-layers of proteins, needs to be taken into account. The charged moieties of the bound proteins along with the counter-ions form a layer that is similar to a ionic gel. The fixed

polyelectrolyte ions generate an electric field that confines the mobile counter-ions in the region of the fixed charges. Eventually a Donnan's equilibrium [21,22,23] is reached where an electrical double layer is formed at the boundary of the fixed ions region (see SI) as sketched in **Figure 2c**. The EGOFET gating system capacitance can therefore be modelled by the following elements in series: a fixed capacitance, C_{fix}, accounting for the HDLs and the PL bilayer capacitance, the $C_{GCDL} \propto \sqrt{i_s}$ and, in the presence of the proteins layer, the Donnan's capacitance that is proportional to the ionic strength ($C_{DON} \propto i_s$).[23] A contribution of a capacitance that is in parallel to the series of elicited elements, C_{par}, is also foreseen to fully account for the staked proteins (see the equivalent circuit in **Figure 2c**). This is expected to be a rather small term (few μF cm^{-2}) that will govern the detection only at very low ionic strength. Overall the gating capacitance C can be described as:

$$\mathbf{C} = \left(\frac{\mathbf{1}}{\boldsymbol{C_{fix}}} + \frac{\mathbf{1}}{\boldsymbol{C_{GCDL}}} + \frac{\mathbf{1}}{\boldsymbol{C_{DON}}}\right)^{\mathbf{-1}} + \boldsymbol{C_{par}} \qquad (5).$$

The binding adds a new layer that changes the capacitance impacting on the $1/C_{DON}$ and also on the C_{par} terms though to a less extent. According to this model, the bio-EGOFET response is indeed governed by a capacitive effect that is *independent from the position* at which the Donnan's equilibrium is set and therefore does not depend on the Debye's length. The latter is expected to dominate in electrostatic, rather than capacitive, detections. To test this hypothesis the dependence of the different terms in equation 5 on the electrolyte ionic strength was studied.

The transfer characteristics of the PL/SA(AV)/Ab and PL/SA(AV)/Ab/CRP EGOFETs gated through PBS solutions at different ionic concentration were measured. **Figures 3a** and **3b** show the response dependence on i_s while the corresponding $\frac{\Delta C}{C_0}$ values are shown in **Figure 3c** and **3d**. The outputs from the solution at the highest i_s = 0.163 M were be taken as

reference. The $\frac{\Delta I}{I_0}$ and $\frac{\Delta C}{C_0}$ data for the EGOFET with the bare PL bilayer are shown for comparison in **Figure 3a and 3c**, respectively. For all the systems the response decreases as i_s decreases and the trend is mirrored by a quantitatively equivalent drop in the capacitance. From **equation 5**, $\Delta C/C_0$ can be written as:

$$\frac{\Delta C}{C_0} = \left(\frac{C_0}{C_{fix}} + \frac{C_0\sqrt{\frac{KT}{e^2\varepsilon\varepsilon^\circ}}}{\sqrt{i_s}} + \frac{C_0 g^{-1}}{i_s} \right)^{-1} + \frac{C_{par}}{C_0} - 1 \qquad (6)$$

where g is the proportionality constant linking the Donnan's capacitance to i_s (see SI). The EGOFET integrating the sole PL lacks the C_{DON} and the C_{par} contributions and, accordingly, the $\Delta C/C_0$ is well described by **equation 6** with $g^{-1}=C_{par}=0$ (black curve in **Figure 3c**). The best fit parameter C_{fix} = 1.3±0.1 μF cm^{-2} is in good agreement with the capacitance of a PL bilayers[24]. The $C_{GCDL} \propto \sqrt{i_s}$ accounts (without any adjustable parameter, see eq. 2) for the 60% decrease in capacitance going from i_s=0.163 M to i_s=1.63x10^{-5} M. For the PL bilayer, the capacitance saturates at high i_s as C_{GCDL} becomes higher than C_{fix}. In the presence of the protein multilayers, $\Delta C/C_0$ saturates also at low i_s because $C_{DON} \propto i_s$ drops already for moderately small ionic strength. Therefore, $\Delta C/C_0$ shows a sigmoidal trend that is well described by **equation 6**. This equation foresees a $\Delta C/C_0$ = -1 at low i_s when C_{par}=0, while the measured values are between -0.4 and -0.8. Apparently, the modeling requires a capacitance in parallel to account for this mismatch. The $\Delta C/C_0$ *vs.* i_s for the protein multilayers have been fitted to **equation 6** (**Figure 3c and 3d** for the SA and the AV-based, respectively) imposing the value C_{fix}=1.3 μF cm^{-2} determined for PL bilayer. As detailed in the SI, the proportionality constant g between the C_{DON} and i_s depends on the volume fraction occupied by the aqueous channel in the protein layer. The binding of the CRP layer drastically reduces this volume fraction by one order of magnitude (see SI) in agreement with the SPR results (**Figure 1b)** indicating a full coverage for the CRP but not for the Ab layer.

In conclusion, we have demonstrated that EGOFET sensors, operated in highly concentrated solutions (λ= 0.7 nm), can sensitively probe a protein binding taking place at more than 20 nm far from the transistor channel. A successful proof-of-principle of their use as sensors directly in serum is also provided. The mechanism of sensing is mainly capacitive and has been ascribed to the formation of Donnan's equilibria within the protein layer originating an extra capacitance in series to the gating system. This capacitive tuning of the EGOFET response is virtually insensible to the Debye's length value. Systematic experiments carried out at different ionic strengths support this model.

Experimental Section

The biotinylated Anti-CRP monoclonal antibody (Ab) and the CRP protein from human plasma were respectively purchased from HyTest and Scripps Laboratories. The human serum fraction was obtained by a blood sample voluntarily donated by one of the authors (G.P.). All other chemicals source, the EGOFET fabrication and functionalization, and the measurement procedures are described elsewhere[11] and detailed also in the SI.

Supporting Information

Supporting Information is available from the Wiley Online Library or from the author.

Acknowledgements

The projects "Sense-of-Care", (EU FP7/2007-2013)., *Nanostructured Soft Matter* (MIUR PRIN 2010-2011) and LABORATORIO SISTEMA (PONa300369 MIUR) are acknowledged for partial financial support. Prof. Paolo Bergese is acknowledged for enlightening discussions.

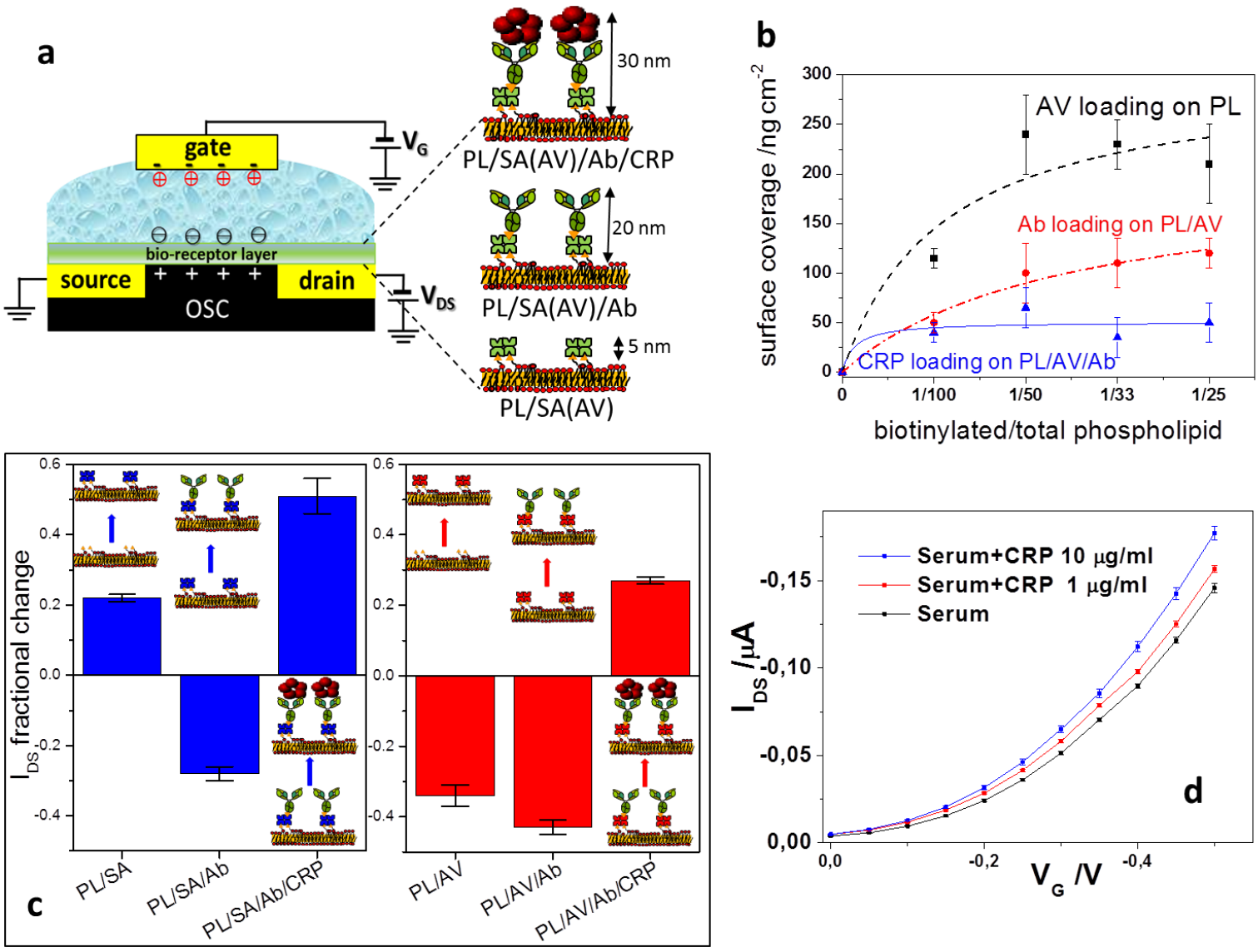

Figure 1

a) Schematic structure of the Bio-EOFET; on the right a sketch of the different multilayers acting as bio-receptor layer.

b) The avidin (AV), antibody (Ab) and CRP surface coverage probed by SPR as a function of the ratio between biotinylated PL and total PL.

c) I_{DS} fractional change upon formation of a new layer (indicated on bottom) for systems based on SA (blue) and AV (red); conditions: V_{DS}= -0.5 V; V_G = -0.5 V; gating solution is PBS at pH=7.4 and i_s=0.163 M.

c) Transfer characteristics for a PL/SA/Ab multilayers, the gating solution was human serum diluted 1/20 v:v with PBS at pH=7.4 and i_s=0.163 M; The diluted serum was either used as blank control (black curve) or loaded with CRP to a final concentration of 1 (red curve) or 10 µg/mL (blue curve).

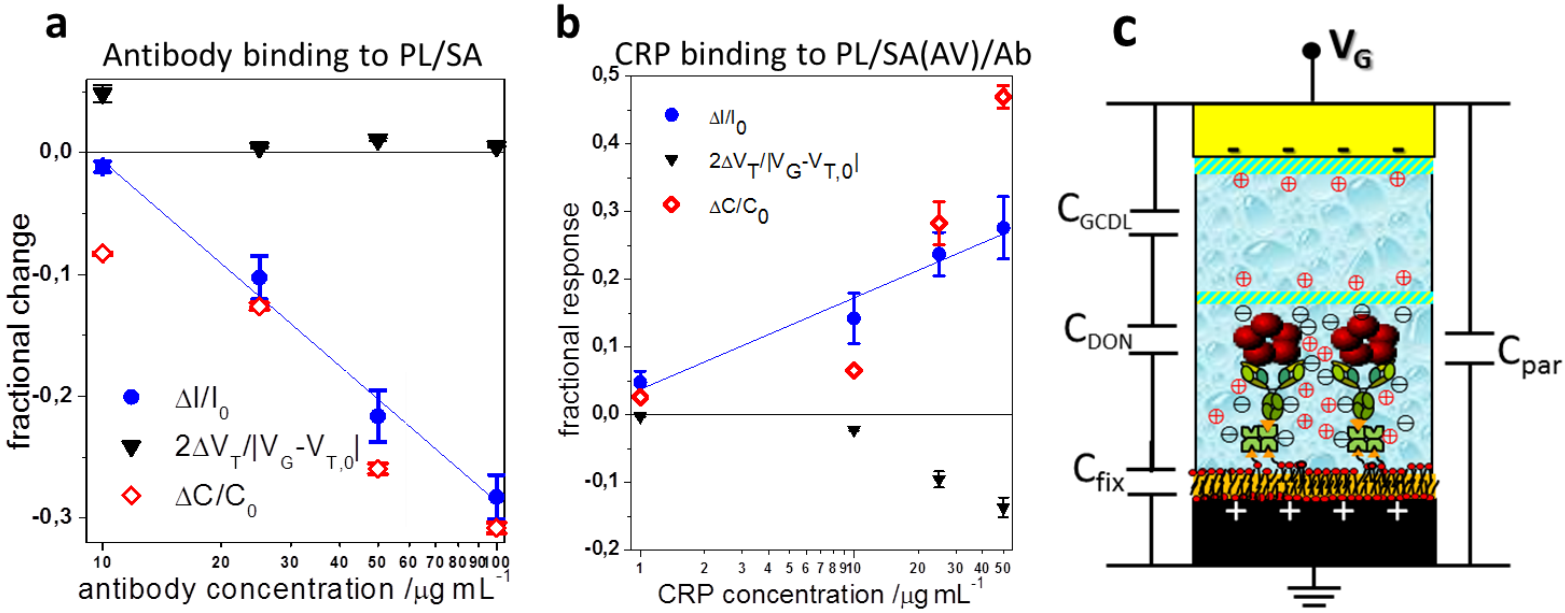

Figure 2

a) Response of PL/SA EGOFET to the loading with Ab (blue dots). The contribution to the response of capacitance (open red diamonds) and V_T changes (black triangles) obtained from the linear interpolation of $\sqrt{I_{DS}}$ *vs.* V_G to equation 3 are also shown.. Data and uncertainties are the mean and standard deviation of at least three measurements. Conditions: V_G=-0.5 V, V_{DS}=-0.5 V the gating solution is PBS at pH=7.4 and i_s=0.163 M.

b) I_{DS}, capacitance and V_T fractional changes of PL/SA/Ab EGOFET to the loading with CRP symbols and conditions as in panel a).

c) Sketch of the charge arrangements in a PL/SA/Ab/CRP multilayer. The dashed regions denote the locations of the ionic double layers. The equivalent circuit of the capacitances involved is also shown.

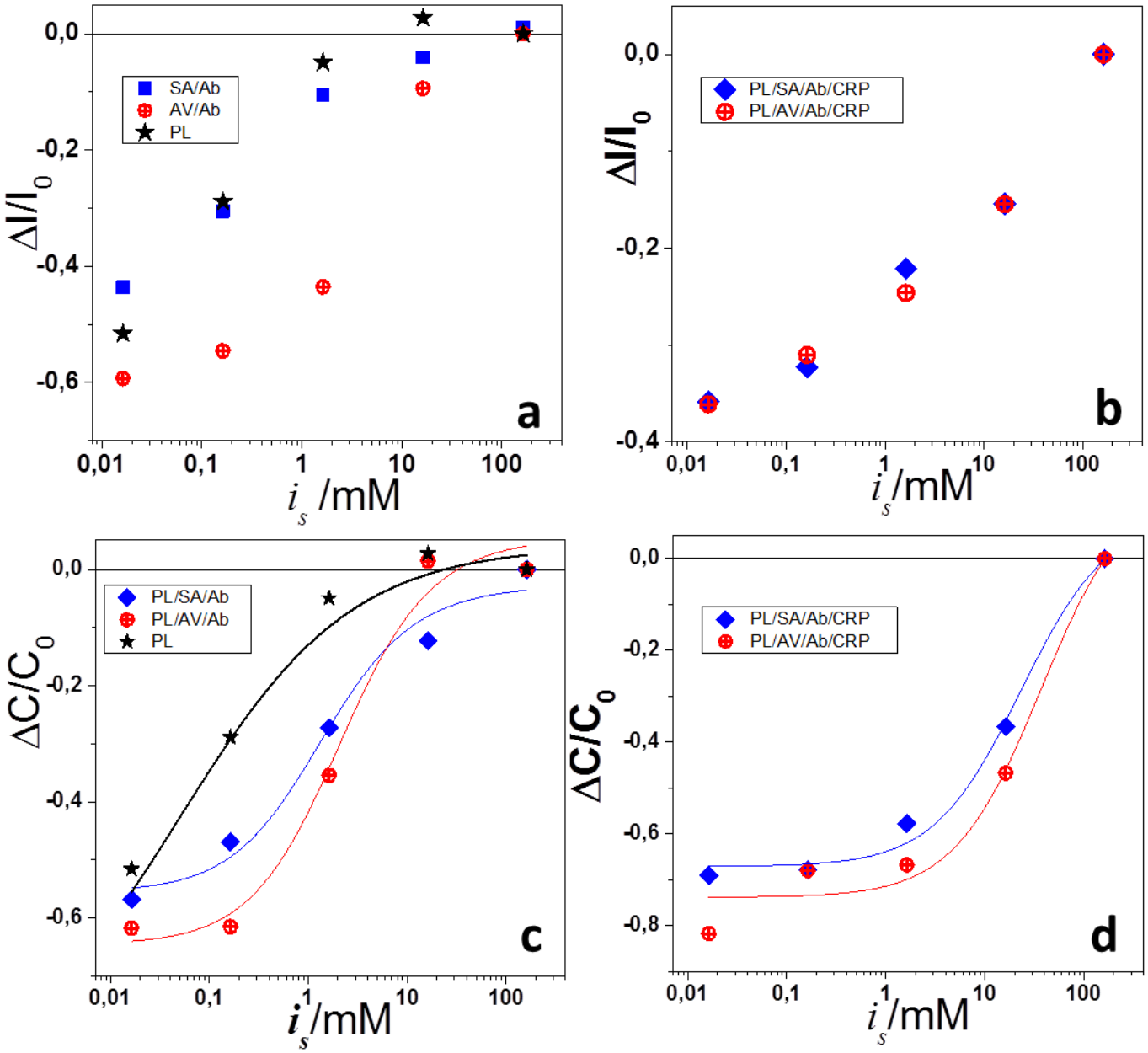

Figure 3
Effect of the ionic strength on the current and capacitance fractional changes of the PL/SA(AV)/Ab (a and c) and the PL/SA(AV)/Ab/CRP (b and d) multilayers. Blue diamonds denote the SA-based systems while the red crossed circles denote the AV-based systems. Also shown as black stars are the current (a) and capacitance (c) data for the bare PL bilayer.The curves are the best fit of the data to equation 6 (same colour code than the symbols). Details on the best-fitting parameters are available in the SI.

[1] Torsi, L., Dodabalapur, A. (2005) Organic Thin-Film Transistors as Plastic Analytical Sensors. *Anal. Chem.*, **77** (19), 380A–387A.
[2] R. M. Owens, G. G. Malliaras, *MRS Bull*. **2010**, 35, 449
[3] J. Rivnay, R.M. Owens, G.G. Malliaras *Chem. Mater*. **2014**, 26, 679.
[4] M. D. Angione , R. Pilolli , S. Cotrone , M. Magliulo , A. Mallardi , G. Palazzo , L. Sabbatini , D. Fine , A. Dodabalapur , N. Cioffi, L. Torsi, *Materials Today* **2011***,* 14*,* 424
[5] M.C. Tanese, D Fine, A Dodabalapur, L. Torsi, *Biosens. Bioelectr.* **2005**, *21*, 782
[6] L. Torsi, M. Magliulo, K. Manoli, G. Palazzo *Chem. Soc. Rev*. **2013,** *42*, 8612-8628.
[7] M.D. Angione, S. Cotrone, M. Magliulo, A. Mallardi, D. Altamura, C. Giannini, N. Cioffi, L. Sabbatini, E. Fratini, P. Baglioni, G. Scamarcio, G. Palazzo, L. Torsi *Proc. Natl. Acad. Sci. USA* **2012**, 109, 6429
[8] A.S. Dhoot, G.M. Wang, D. Moses, H.J. Heeger, *Phys. Rev. Lett.* **2006**, *96*, 246403
[9] M.J. Panzer, C.D. Frisbie, *Appl. Phys. Lett* **2006**, *88*, 203504.
[10] K. Melzer, A.M. Münzer, E. Jaworska, K. Maksymiuk, A. Michalska, G. Scarpa, *Org. Electron*. **2014**, 15, 595.
[11] M. Magliulo, A. Mallardi, M. Yusuf Mulla, S. Cotrone, B.R. Pistillo, P. Favia, I. Vikholm-Lundin, G. Palazzo, L Torsi, *Adv. Mater.* **2013**, 25, 2090
[12] J. Israelachvili Intermolecular and surface forces. Academic Press, London, UK, **1992** chpt.14
[13] E. Stern, R. Wagner, F.J. Sigworth, R. Breaker, T.M. Fahmy, M.A. Reed, *Nano Lett.* **2007**, 7, 3405
[14] F.N. Ishikawa, M.Curreli, H-K. Chang, P-C. Chen, R. Zhang, R.J. Cote, M.E. Thompson, C. Zhou, *ACS-nano*, 2009, 12, 3969
[15] M.L. Hammock, O. Knopfmacher, B.D. Naab, J.B-H. Tok, Z. Bao, *ACS-Nano*, **2013**, 7, 3970
[16] W. Huang, K. Besar, R. LeCover, P. Dulloor, J. Sinha, J.F. Martìnez Hardigree, C. Pick, J. Swavola, A.D. Everett, J. Frechette, M. Bevan, H. E. Katz, *Chem. Sci*. **2014**, 5, 416
[17] O. Knopfmacher, M.L. Hammock, A.L. Appleton, G. Schwartz, J. Mei, T. Lei, J. Pei, Z. Bao, *Nature Comm*., **2014**, 5 art. 2954
[18] N.M. Green, *Methods Enzymol*. **1990**, *184*, 51.
[19] J.N. Herron, H-K Wang, V. Janatova, J.D. Durtschi, D.A. Christensen in *Biopolymers at Interfaces* (Ed M. Malmstein) Marcel Dekker, New York , **2003**, Ch. 6.
[20] E. Stern, J. F. Klemic, D. A. Routenberg, P. N. Wyrembak, D. B. Turner-Evans, A. D. Hamilton, D. A. LaVan, T. M. Fahmy, M. A. Reed, *Nature*, **2007**, 445, 519
[21] H. Ohshima *Sci. Technol. Adv. Mater.* **2009**, 10, art. 063001
[22] Ohshima H *Theory of Colloid and Interfacial Electric Phenomena,* Elsevier/Academic Press, New York, USA **2006**
[23] M. Borkovec, B. Jönsson, G.J.M. Koper in *Surface and Colloid Science*, Vol. 16 (Ed. E. Matijevic) p.99 Kluwer, New York, USA 2001, Ch.2
[24] A.L. Plant, M. Gueguetchkeri, W. Yap, *Biophys. J*., **1994**, 67, 1126,